# Implementation of Adaptive Antenna Array for Ground Station Tracking System

By Syazana Basyirah MOHAMMAD ZAKI,[1,3] Nobuyuki KAYA,[2] and Mengu CHO[1]

[1]*Laboratory of Spacecraft Environment Interaction Engineering, Department of Applied Science with Integrated System Engineering, Kyushu Institute of Technology, Japan*

[2]*WaveArrays, Inc., Kobe University, Japan*

[3]*Center of Satellite Communication, Faculty of Electrical Engineering, Universiti Teknologi MARA, Shah Alam, Selangor, Malaysia*

(Received June 21st, 2019)

As the number of small satellites keeps increasing due to the low-cost development and fast delivery duration, there is a demand for higher capacity and capability of the ground station tracking system. Generally, the existing ground station tracking system faces major performance degradation while tracking satellites because of signals interference and multi-path fading. These problems motivate researchers to come out with interesting solution to mitigate the degradation performance. This paper describes the implementation of adaptive beam forming algorithm of phased array antenna for ground station tracking system. The adaptive antenna array demonstrates electronically self-steering radiation pattern capability towards satellites signals, suppress interferences and multi-path signals. This can be achieved by adapting the Least Mean Square (LMS) algorithm by varying the number and phase of the array antenna elements and the angle of beam steering to determine the Direction of Arrival (DOA) of incoming signals. The performance of adaptive LMS algorithm is investigated in MATLAB software by analyzing the radiation patterns for different number of array antenna elements, phases and beam steering angle. The purpose of LMS algorithm implementation in the Adaptive Array Antenna (AAA) system is to control weights adaptively, optimize the Signal to Noise Ratio (SNR) of the desired signal and minimize the Mean Square Error (MSE).

**Key Words:** Adaptive Antenna Array, Adaptive Beamforming, Least Mean Square algorithm

**Nomenclature**

| | | |
|---|---|---|
| $P$ | : | point of observation |
| $t$ | : | time, second |
| $r$ | : | distance to point of observation, $P$ |
| $d$ | : | inter-element distance between antenna |
| $\lambda$ | : | wavelength of the received signal |
| $N$ | : | total number of array antenna element |
| $A$ | : | amplitude of the received signal |
| $\phi$ | : | phase difference between incident waves |
| $\mu$ | : | step-size |
| $k$ | : | $k^{th}$ sampling instant |
| $\beta$ | : | phase propagation factor |
| $\theta$ | : | angle of arrival signal, degree |
| Subscripts | | |
| $N$ | : | total number of antenna elements |
| $c$ | : | carrier |
| $i$ | : | number for each array antenna element |
| $x$ | : | $x$ plane |
| $y$ | : | $y$ plane |

## 1. Introduction

As the number of small satellites constellation launched to the Low Earth Orbit (LEO) keeps increasing due to low-cost development and fast delivery duration, the demands of higher capacity and capability of a Ground Station (GS) tracking system are also growing. The communication with a LEO satellite constellation has the advantages of shorter transmission delays, small path losses, low-cost, and low-power ground terminals [1] with respect to Medium Earth Orbit (MEO) and Geo Stationary Orbit (GEO). Because of those advantages, it gives an impact on the saturation of data capacity downloaded from satellites to GS and vice-versa [2]. However, the conventional GS which integrate the control segment of a satellite mission, commonly has large dishes antennas for space communication. Apart from expensive (high cost of operation and maintenance), mechanical complexity of steering (back and forth) and slow movement are the significant constraints which lead to the incapability of satellites multi-target tracking.

Another limitation of the conventional GS is the antenna systems unable to isolate source signals from complex interference environments such as source signals from other satellites and other signal sources. The deployment of satellite constellations at LEO bring a serious in-line interference problem to the satellite constellations network in the higher orbit. In [1], Mendoza et al., (2017) discussed on the analysis of in-line interference of a LEO satellite passes through a line of sight path between a GS and a GEO satellite. Besides, multipath-fading signal also occurs to the conventional ground-to-satellite/satellite-to-ground communication link. It gives a degradation impact towards its performance (degradation of system capacity) [3] when the omnidirectional signal generated by the satellites reflected and scattered by surroundings (such as structures, buildings and mountains); resulting in the arrival of multiple delayed (multipath) of the main signal (direct signal) before arriving at the GS. As the signal delayed, the

phases of the multipath signal components can be destructively over a narrow bandwidth, leading to fading of the received signal level and self-interference; resulting in a reduction of the signal strength.

A constellation of small satellites launched to the LEO are mostly orbiting around the Earth in between the altitude of 400 km to 2000 km. Within this range of altitudes, the velocity of a satellite relative to a fixed observer is very high. The satellite visibility duration on the footprint is about 10 to 20 minutes. Due to this mobility, a proper beam steering and fast-switching tracking system for small satellites is needed. Kyun et al., (2002) stated in [4], a phased array antenna with electronic steerable beam scanning is the most promising solution.

To mitigate all above-mentioned constraints, an Adaptive Antenna Array (AAA) system or also known as Smart Antenna system which implement LMS algorithm is simulated in this paper. It is also described as a phased antenna array that implements Digital Signal Processing (DSP) in its system. The antenna GS system is expected to improve the performance of conventional GS to serve as the gateway for satellite tracking and telemetry and command (TT&C) operation. In the simulation results and analysis in Section 5, the results show the ability of the adaptive algorithm to perform fast-tracking (main beam could be steered every 2.5 seconds) to be able to track multiple moving constellation satellites. Furthermore, the proposed AAA GS system has the ability to enhance signal quality through multi-target capability, where it can track different satellites (constellation satellites) simultaneously, by dividing the array into sub-arrays with simultaneous beamforming processes for fast-tracking.

### 1.1. Adaptive array antenna for GS tracking system

The objectives of this research are to demonstrate the capability of electronically self-steering radiation pattern and determine the Direction-of-Arrival (DOA) of incoming signals. The AAAs can adapt the signal environment, reduce delay spread and multipath fading, thereby increasing capacity by improving link quality. They can tailor themselves to the signal environment and exploit or reject the reflected signal. It can be accomplished by optimizing the Signal-to-Interference Ratio (SIR) at the array output. Thus, the AAA systems are incredibly effective for radar application and communication systems for protection from interference and jamming.

The implementation of AAA in a GS for satellites tracking system has the ability to perform a directional radiation beam steering towards the satellite signal while nulling out the interference signals. Satellites will dynamically able to be tracked, and beam steering will be controlled electronically by the system to point the main beam only, and only towards the desired satellite. The inter-element spacing, relative phase and amplitudes which fed to each array antenna elements are the main factors that contribute to the radiation pattern radiated by individual element, hence finally affects the overall radiation pattern of all array antenna elements.

### 1.2. Least mean square algorithm

The LMS algorithm was introduced by Widrow and Hoff in 1959 which uses a gradient-based method of steepest descent to minimize the MSE between the desired signal and the array output signal [5]. The LMS algorithm was adapted in the AAA control system because of its simplicity, ease of computation (does not need memory and matrix inversion) [6] and it was found to be the best choice for different applications of adaptive signal processing [7]. Not limited to demonstrate the capability of self-steering beamforming and to minimize the MSE of the error signal, LMS algorithm was implemented in the AAA system to provide the best possible estimation with each iteration until the weight has adapted or converged. An optimum set of weighting factors is determined to maximize the power of the desired signal or Signal-of-Interest (SOI) while minimizing the noise and interference or Signal-of-Not-Interest (SNOI). The performance of the LMS algorithm was verified by simulation in MATLAB software.

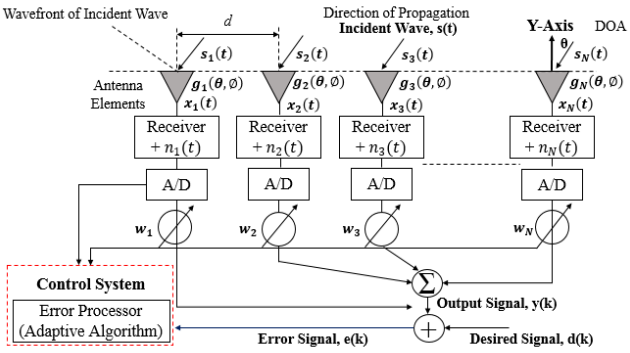


Fig. 1. LMS beamforming network [8] [9].

Generally, in the design of array architecture, the overall array radiation pattern is obtained from the radiation pattern of individual elements (include gain, $g_N(\theta, \emptyset)$), their positions, orientation in space, relative amplitude and phase of feeding currents to the elements. Steerable direction capability (without physically move any of individual elements) towards the desired user is achievable by varying amplitude and phase of individual elements output before the combining process. Figure 1 shows the diagram of adaptive array architecture which is based on the LMS algorithm. Due to the difference in distance traveled by the wave between two antenna elements, the signals incident on all the antenna elements are in different phases. The signal present at Element #1 has traveled more distance $dsin(\theta)$ than signal present at Element #2, affected the phase of Element #1 lags behind Element #2 by $\beta dsin(\theta)$. where

$d$: Distance between successive antenna phase centers in the array

$\beta$: Phase propagation factor $= 2\pi/\lambda$

$\lambda$: Wavelength of received signal

As the incident waves, $\mathbf{s}(t)$ arriving at antenna elements; electrical signals (incoming signals), $\mathbf{x}(t)$ is then down-converted by the receiver from Carrier Frequency, $f_c$ to an Intermediate Frequency (IF). The IF is sampled by an Analog to Digital (A/D) converter to convert the electrical signals (incoming signals), $\mathbf{x}(t)$ into input signals, $\mathbf{x}_i(t)$ from analog to digital form signal as the waves reach the antenna elements.

By referring to the diagram in Figure 1, input signals, $\mathbf{x}_i(t)$, defined as $\mathbf{x}_1(t)$ , $\mathbf{x}_2(t)$ ,…… $\mathbf{x}_N(t)$ are multiplied with input weight (adjustable weights), $\mathbf{w}_1$ , $\mathbf{w}_2$ ,…… $\mathbf{w}_N$ . The modification of amplitude and phase is applied during the multiplication process of each antenna element input signals, $\mathbf{x}_i(t)$ with input weights, $\mathbf{w}_i$. All the symbols are summed to produce an output signal (received signal), $\mathbf{y}(t)$ . In mathematical form, general equation of adaptive beamforming process can be written as in Equation (1) [8] [9] [10]:

$$\mathbf{y}(t) = \sum_{i=1}^{N} \mathbf{x}_i(t)\mathbf{w}_i. \quad (1)$$

where

$\mathbf{y}(t)$: Output signal
$N$: Number of antenna elements
$\mathbf{x}_i(t)$: Input signals
$\mathbf{w}_i$: Input weights

LMS algorithm is an adaptive beam-forming algorithm for tuning the required signal and rejecting the interfering signal at the antenna array. It is one of the most popular adaptive algorithm in Temporal-Reference algorithm (one type of beamforming technique algorithm). Based on Temporal-Reference algorithm, a known reference signal (desired signal), $\mathbf{d}(t)$ is required to be included in the frame of the signal. In this AAA case, $\mathbf{d}(t)$ is actually the signal from the tracked satellite. Aims of using beamforming technique algorithm is to minimize the energy of an error signal integrated by interferences and noises. Iterative procedure for weight calculation leads to MSE, mathematically can be calculated as [6]:

$$\mathbf{y}(t) = \sum \mathbf{s}_i(t)\mathbf{a}(\theta)' + \sum \mathbf{I}_i(t)\mathbf{a}(\theta)'' + \mathbf{n}(t). \quad (2)$$

where

$i$: Number for each array antenna element from 1 to $N$
$N$: Total number of array antenna element
$\mathbf{y}(t)$: Antenna array output
$\mathbf{s}_i(t)$: Received signal from satellite
$\mathbf{a}(\theta)'$: Steering vector for desired direction
$\mathbf{I}_i(t)$: Interference signal
$\mathbf{a}(\theta)''$: Steering vector for undesired direction
$\mathbf{n}(t)$: Noise signal in the receiver channel connected to each antenna element (Gaussian noise with zero mean)

Noise is modeled by $\mathbf{n}(t) = [\mathbf{n}_1(t)\mathbf{n}_2(t) \ldots \mathbf{n}_N(t)]$, a $1 \times N$ row vector of complex white noise with variance, $\sigma^2$. The assumption is that each of the transmitted signals and noise sequences are mutually uncorrelated. The error processor computes the required weight adjustment to null out the undesired signal by iterative process and will continue until all the weights in the array converge. The adaptive algorithm is exploited to minimize the error signal, $\mathbf{e}(t)$ between the reference signal (desired signal), $\mathbf{d}(t)$ and the received signal, $\mathbf{y}(t)$ which can be written as in Equation (3):

$$\mathbf{e}(t) = \mathbf{d}(t) - \mathbf{y}(t). \quad (3)$$

A narrow band incident wave (received signal), $\mathbf{s}(t)$ which arrives at antenna elements is written as in Equation (4):

$$\mathbf{s}(t) = Aexp(2\pi f_c t + \emptyset). \quad (4)$$

where

$A$: Amplitude of the received signal
$f_c$: Carrier Frequency
$\emptyset$: Phase difference between incident waves at successive elements $= 2\pi/\lambda dsin(\theta)$

By taking received signal at Element #1 as the reference, the received signals, $\mathbf{x}_i(t)$ for uniform linear array with element spacing, $d$ is represented in matrix form as in Equation (5) [10]:

$$\mathbf{x}_i(t) = \begin{bmatrix} 1 \\ exp[-j\beta dsin(\theta)] \\ \vdots \\ exp[-j\beta(N-1)dsin(\theta)] \end{bmatrix} \mathbf{s}(t), \quad (5)$$

which can be simplified as Equation (6)

$$\mathbf{x}_i(t) = \mathbf{a}(\theta)\mathbf{s}(t). \quad (6)$$

where

$N$: Number of antenna elements
$\theta$: Angle of arrival with respect to Y-axis
$\mathbf{a}(\theta)$: Steering vector which control direction of antenna beam at angle-of-arrival, $\theta$

By inserting Eq. (5) into Eq. (1), yield Equation (7)

$$\mathbf{y}(t) = [\mathbf{w}_1, \mathbf{w}_2, \ldots \mathbf{w}_N] \begin{bmatrix} 1 \\ exp[-j\beta dsin(\theta)] \\ \vdots \\ exp[-j\beta(N-1)dsin(\theta)] \end{bmatrix} \mathbf{s}(t) \quad (7)$$

which can be simplified as in Equation (8)

$$\mathbf{y}(t) = \mathbf{w}_i\mathbf{x}^T(t). \quad (8)$$

The overall antenna pattern is continuously modified by adjusting weight vector. For digital communication system, the input signals are in discrete time sampled data form. Therefore, the output signal will be as in Equation (9):

$$\mathbf{y}(k) = \mathbf{w}_k\mathbf{x}^T(k). \quad (9)$$

where

$k$: $k^{th}$ sampling instant

### 1.3. LMS Weight Equation Derived from Steepest Descent algorithm

Steepest descent method based on gradient-based is implemented in the LMS algorithm to update the weights in order to avoid the direct matrix inversion and minimize the MSE. Basic description of LMS algorithm is as in Equation (10) and Equation (11) [8]:

$$\mathbf{e}(k) = \mathbf{d}(k) - \mathbf{w}(k)\mathbf{x}^T(k). \quad (10)$$

$$\mathbf{w}(k+1) = \mathbf{w}(k) - \mu\nabla\xi(k). \quad (11)$$

where

$\mathbf{e}(k)$: Error signal between the reference signal and the output signal (applied in case of SOI and SNOIs)
$\mathbf{w}(k)$: Value of weight vector before adaptation at time, $k$
$\mathbf{w}(k+1)$: Value of weight vector after adaptation (updated weight) at time, $k$
$\mu$: Step-size which controls the speed of convergence
$\nabla\xi(k)$: Gradient of the cost function

which

$$\xi(k) = \mathbf{E}[\mathbf{e}^2(k)], \quad (12)$$

where

$\mathbf{E}$ is the expectation error signal (unknown), and therefore instantaneous value is used as an estimation. Therefore, Equation (12) becomes Equation (13):

$$\xi(k) = [\mathbf{e}^2(k)], \quad (13)$$

where

$\mathbf{e}^2(k)$ is the MSE between beamforming output signal, $\mathbf{y}(k)$ and the reference signal, $\mathbf{d}(k)$. By referring to Eq. (12), the

derivation of the gradient of cost function, $\nabla\xi(k)$ becomes as in Equation (14):

$$\nabla\xi(k) = -2\mathbf{e}(k)\mathbf{x}(k), \quad (14)$$

by substituting the Eq. (14) into the general equation of Steepest Descent algorithm in Eq. (11), yield Equation (15):

$$\mathbf{w}(k+1) = \mathbf{w}(k) + 2\mu\mathbf{e}(k)\mathbf{x}(k). \quad (15)$$

The tap weight of the vector is updated in preparation for the new sample/next iteration by the Eq. (15); where $\mathbf{w}(k)$ is the weight vector before adaptation at time, $k$, while $\mathbf{w}(k+1)$ is the weight vector after adaptation at time, $k$. $\mu$ is the step-size or gain constant which controls the convergence characteristics of the LMS algorithm. The LMS algorithm is initiated with some initial weights, to converge and stay stable, the $\mu$ value should be within the limit of $0 < \mu < \frac{1}{\lambda_{max}}$, where $\lambda_{max}$ is the maximum Eigen value of the input covariance matrix. According to (Breslin, 1997) in [10], if $\mu$ is chosen to be very small value, then the algorithm converges very slowly. Otherwise, a large value of $\mu$ may lead to a faster convergence but may be less stable around the minimum value [8]. Proper technique of choosing the $\mu$ value is by firstly use the maximum allowed value, and once the change in error is stabilized, the $\mu$ is reduced to reach the best result. $\mathbf{e}(k)$ is known as the error estimation and $\mathbf{x}(k)$ is the input vector of time delayed input values.

This paper is structured as follows. Section 1 describes the objectives and the importance of implementation of AAA for GS tracking system. General concept, related derivation equations and beamforming network of LMS algorithm in AAA are explained in Section 1.2 until Section 1.3. Section 2 contains the array factor of planar array geometry and its related equation. Orbital simulation and satellite constellation on the same orbital plane or different orbital plane which are simulated in Systems Tool Kit (STK) software is presented in Section 3. Systems Tool Kit formerly known as Satellite Tool Kit and often referred to by its initials which is STK. STK is a physics-based software package from Analytical Graphics, Inc. that allows us to perform complex analyses of ground to space platforms and share results in one integrated environment. The space tools in STK can help with system architecture, trajectory design, orbit determination and subsystem analysis. The simulation of orbital model and LEO satellite constellation interference and analysis on different scenarios of LEO constellations are discussed in Section 4. Section 5 presents the simulation results of LMS algorithm and the analysis of its performance is also discussed in this section. There is a suggestion on the improvement of the LMS algorithm in the Conclusion in Section 6.

## 2. Array factor of planar array geometry

Array factor (AF) is a function of weights, positions and steering vector use in the antenna array or phased array. This factor quantifies the effect of combining radiating elements in an array without the element specific radiation pattern taken into account. It is based on interference between the radiated fields of the elements in the array. The manipulation of the weights will allow the AF to be tailored to a desired pattern. The response of AF is strongly influenced by specified geometry used which in this research, it is a planar array geometry. Planar array antenna (considering $M \times N$ isotropic elements) geometry is commonly used in AAA as it has the capability of steering/scanning the main beam towards any desired direction (at maximum radiation and reception in both azimuth, $\emptyset$ and elevation, $\theta$) [3]. Moreover, planar array antenna is more versatile as it provides more symmetrical patterns with lower side lobes, much higher directivity (narrow main beam).

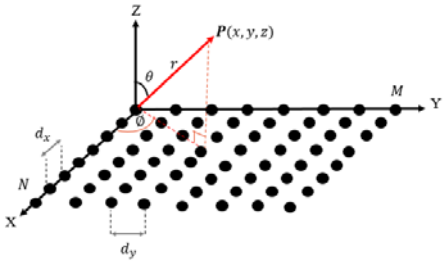


Fig. 2. Planar array geometry.

Based on planar array factor geometry in Figure 2, a general equation of planar array factor is as calculated in Equation (16):

$$AF = AF_x AF_y = \sum_{m=1}^{M}\sum_{n=1}^{N} \mathbf{w}_{mn} e^{j[(m-1)(\Psi_x+\beta_x)+(n-1)(\Psi_y+\beta_y)]} \quad (16)$$

where

$\mathbf{w}_{mn}$ = Complex array weight at element $m$, $n$

$\Psi_x = kd_x sin_\theta cos_\emptyset$

$\Psi_y = kd_y sin_\theta sin_\emptyset$

$\beta_x = -kd_x sin_\theta cos_\emptyset$

$\beta_y = -kd_y sin_\theta sin_\emptyset$

where

$k$ = Wave number ($2\pi/\lambda$)

$d_x, d_y$ = Inter-element spacing for $x$, $y$

$\theta$ = Angle of incidence of electromagnetic plane wave from array axis

$\emptyset$ = Angular position of $m^{th}$, $n^{th}$ elements on $x$, $y$ plane

## 3. Orbital simulation and satellites constellations

The real-time scenario of different LEO satellite constellations was simulated in STK software. The Two-Line Element (TLE) orbital data was imported from public online satellite databases [11]. The scenario under analysis is composed by three satellites constellations launched from January 12th to June 29th, 2018 which involving three units of 1U CubeSats constellation from BIRDS-2 Project, four units of 3U CubeSats constellation from Planet Lab and four units of 3U CubeSats from Spire Global, Inc. The orbital analysis processes the interference towards inter-satellite constellation (on the same or different orbital plane) from the point of view of BIRDS GS at Kyushu Institute of Technology (Kyutech), Japan from January 9th, 2019 (03:00:00 UTC) until January 10th, 2019 (03:00:00 UTC). BIRDS GS is located at 33.89° N and 130.84° E with antenna boresight direction pointing to the BIRDS-2, FLOCK-3P' and LEMUR-2 CubeSats. From this analysis, three different

scenarios of constellations are created in STK, considering satellite constellations on the same or different orbital plane.

- Constellation #1 (BIRDS-2 1U CubeSats): Having number of CubeSats, $N_S = 3$, located at altitude, $H = 408$ km on 1 orbital plane (all 3 CubeSats are on the same orbital plane), with inclination, $i = 51.6°$ over the equatorial plane.
- Constellation #2 (FLOCK-3P' 3U CubeSats): Having number of CubeSats, $N_S = 4$, located at altitude, $H = 522$ km on 1 orbital plane (all 4 CubeSats are on the same orbital plane), with inclination, $i = 97.5089°$ over the equatorial plane.
- Constellation #3 (LEMUR-2 3U CubeSats): Having number of CubeSats, $N_S = 4$, located at altitude, $H = 492$ km on 1 orbital plane (all 4 CubeSats are on the same orbital plane), with inclination, $i = 97.5077°$ over the equatorial plane.

## 4. Scenario under analysis

### 4.1. Scenario I

The first real-time scenario occurs on January 9th, 2019 at 21:54:39 UTC involving Constellation #1 where BHUTAN-1 CubeSat is the targeted satellite while MAYA-1 and UiTMSAT-1 CubeSats act as interferers. Figure 3(a) shows the Constellation #1 scenario: 3D orbital simulation of BIRDS-2 satellites constellation on the same orbital plane simulated in STK software.

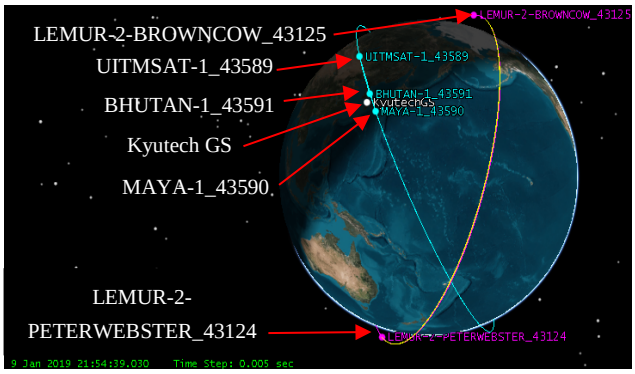


Fig. 3(a). 3D orbital simulation of BIRDS-2.

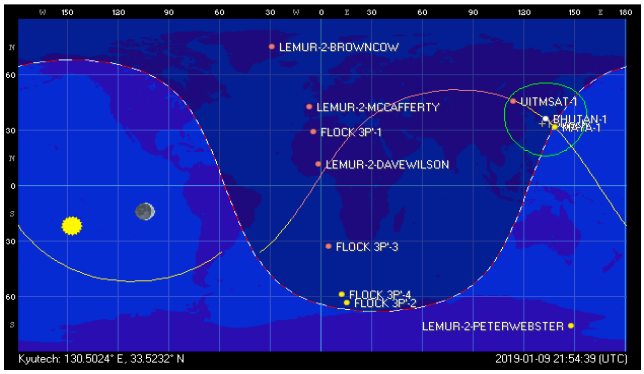


Fig. 3(b). 2D orbital simulation of BIRDS-2.

MAYA-1 is estimated to be the first satellite passes the Kyutech GS, continued by BHUTAN-1 and UiTMSAT-1. The Acquisition of Signal (AOS) and Loss of Signal (LOS) of Constellation #1 passes are predicted by using Orbitron software, considering satellites elevation are 10° and higher. The Constellation #1 sequence started with MAYA-1 CubeSat to enter the Kyutech GS footprint and ends with UiTMSAT-1 CubeSat. BHUTAN-1 CubeSat (targeted satellite) entered the Kyutech GS footprint at AOS of 21:49:16 UTC and leaved the footprint at LOS of 21:58:52 UTC. This AOS and LOS time are chosen according to the prediction of BHUTAN-1 CubeSat at the maximum elevation angle of 28° during the pass. Figure 3(b) shows the 2D orbital simulation of BIRDS-2 satellites constellation in Orbitron software.

### 4.2. Scenario II

The second real-time scenario involves the Constellation #2 which took place on January 9th, 2019 at 12:52:45 UTC involving FLOCK-3P'-4 CubeSat as the targeted satellite while FLOCK-3P'-2 and FLOCK-3P'-3 CubeSats act as interferers. Figure 4(a) shows the Constellation #2 scenario: 3D orbital simulation of FLOCK-3P'satellites constellation on the same orbital plane simulated in STK software. FLOCK-3P'-3 is estimated to be the first satellite passes the Kyutech GS, continued by FLOCK-3P'-4 and FLOCK-3P'-2. Figure 4(b) shows the 2D orbital simulation of FLOCK-3P' satellites constellation in Orbitron software. The AOS and LOS of the Constellation #2 are between 12:41:38 and 13:01:27 UTC with the sequence of satellites started with FLOCK-3P'-3 CubeSat and ends with FLOCK-3P'-2 CubeSat. The targeted satellite is FLOCK-3P'-4 at the maximum elevation angle of 89° during the pass.

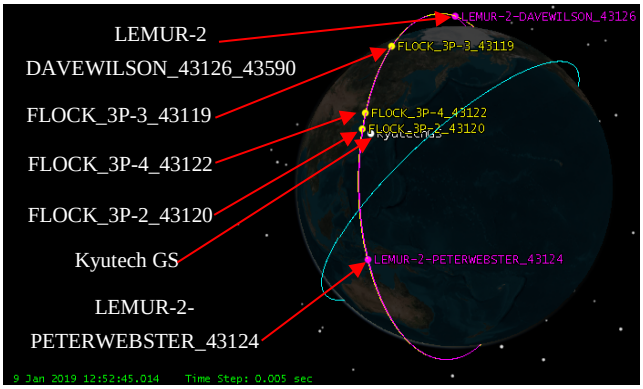


Fig. 4(a). 3D orbital simulation of FLOCK-3P'.

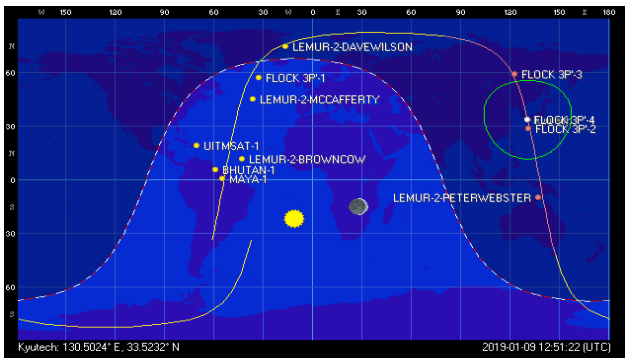


Fig. 4(b). 2D orbital simulation of FLOCK-3P'.

### 4.3. Scenario III

The third real-time scenario occurs on January 9th, 2019 at 12:28:24 UTC involving Constellation #2 and Constellation #3 where FLOCK-3P'-1 CubeSat is the targeted satellite while LEMUR-2-MCCAFFERTY and LEMUR-2-DAVEWILSON CubeSats act as interferers. Figure 5(a) shows the Constellation #2 and Constellation #3 scenario: 3D orbital simulation of FLOCK-3P' and LEMUR-2 satellites constellation on different orbital plane simulated in STK software. For the third scenario, the sequence pass involving two different satellites constellations on different orbital plane, LEMUR-2-MCCAFFERTY is estimated to be the first satellite passes the Kyutech GS footprint, continued by FLOCK-3P'-1 and LEMUR-2-DAVEWILSON. FLOCK-3P'-1 CubeSat (targeted satellite) entered the Kyutech GS footprint at AOS of 12:29:57 UTC and left the footprint at LOS of 12:41:26 UTC. This AOS and LOS time are chosen according to the prediction of FLOCK-3P'-1 CubeSat at the maximum elevation angle of 47° during the pass. Figure 5(b) shows the 2D orbital simulation of FLOCK-3P' and LEMUR-2 satellites constellations in Orbitron software.

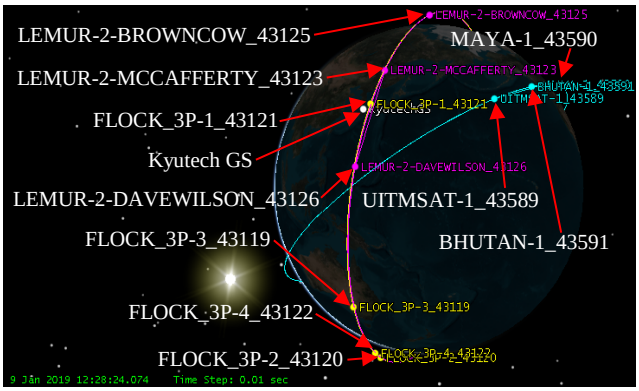


Fig. 5(a). 3D orbital simulation of FLOCK-3P' and LEMUR-2.

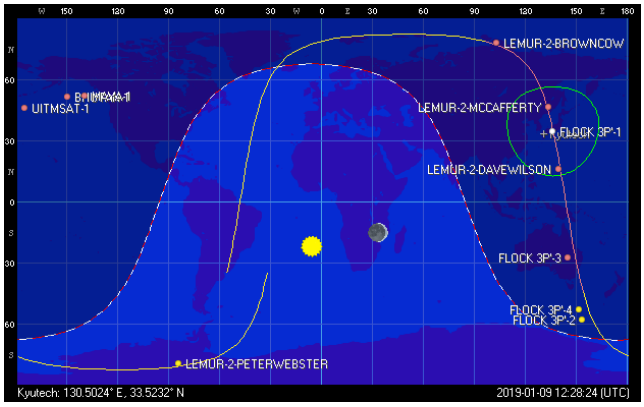


Fig. 5(b). 2D orbital simulation of FLOCK-3P' and LEMUR-2.

### 4.4. Scenario analysis

According to the Report Access: AER (Azimuth, Elevation and Range) generated in the STK orbital simulation, precise locations of satellites under analysis are determined. By referring to the planar array geometry in Figure 1, the phi, $\emptyset$ represents the azimuth (degree), the theta, $\theta$ represents the elevation (degree) and $R$ represents the range (km) from the observation point, $P$. Objects (Satellites Under Analysis) are accessed from the Kyutech GS.

The generated Report Access analysis for Scenario I, II and III are as stated in Table 1. Based on the information generated from the Report Access in Table 1, the AER data are used in the simulation of LMS algorithm in MATLAB simulation software for interference analysis. The presence of interferers is evaluated by considering three radiation patterns; main lobe (towards targeted satellite) and side lobes (towards interferer satellites).

Table 1. Report access: AER of scenario I, II and III for CubeSats.

| Scenario | CubeSats | AOS, Time (max elevation), LOS (UTC) | A(°), E(°), R(km) for each CubeSat at each AOS, maximum elevation and LOS |
|---|---|---|---|
| I | BHUTAN-1 | 21:49:16 | 323, 0, 2361 |
| | | 21:54:21 | 37, 28, 784 |
| | | 21:58:52 | 112, 0, 2346 |
| | MAYA-1 | 21:47:30 | 325, 0, 2364 |
| | | 21:54:35 | 35, 21, 943 |
| | | 21:58:52 | 105, 0, 2349 |
| | UiTMSAT-1 | 21:53:53 | 322, 0, 2366 |
| | | 21:54:59 | 37, 28, 780 |
| | | 22:04:37 | 112, 0, 2344 |
| II | FLOCK-3P'-4 | 12:46:54 | 168, 0, 2634 |
| | | 12:52:45 | 245, 89, 349 |
| | | 12:58:37 | 349, 0, 2637 |
| | FLOCK-3P'-2 | 12:49:45 | 169, 0, 2628 |
| | | 12:55:35 | 256, 81, 506 |
| | | 13:01:27 | 348, 0, 2636 |
| | FLOCK-3P'-3 | 12:41:38 | 164, 0, 2630 |
| | | 12:47:28 | 78, 76, 513 |
| | | 12:53:19 | 351, 0, 2635 |
| III | FLOCK-3P'-1 | 12:29:57 | 156, 0, 2621 |
| | | 12:35:41 | 75, 47, 661 |
| | | 12:41:26 | 356, 0, 2632 |
| | LEMUR-2-MCCAFFERTY | 12:24:01 | 153, 0, 2632 |
| | | 12:29:44 | 78, 41, 735 |
| | | 12:35:27 | 357, 0, 2636 |
| | LEMUR-2-DAVEWILSON | 12:31:32 | 156, 0, 2619 |
| | | 12:37:16 | 76, 49, 636 |
| | | 12:43:02 | 355, 0, 2629 |

## 5. Simulation results and analysis

The MATLAB simulation is performed to analyze the results of the LMS algorithm by optimizing and computing weights and beamforming patterns. A uniform $8 \times 8$ elements of a planar antenna array with individual elements spaced at half-wavelength $(0.5\lambda)$ distance is fixed parameter in this simulation. The LMS simulation in MATLAB uses input parameters of satellite's elevation and azimuth in Table 1 which involving three scenarios of satellites constellations. In the

simulation, the number of SOI (targeted signal) and SNOIs (interferer signals) are set as default parameters, which indicates as one particular satellite (meant to be tracked) and two other satellites which act as interferers. In order to achieve maximum ratio of desired signal strength to the interferer signal strength, 'Step-size value' ($Mu$ ($\mu$)), 'Additive Noise' (Mean of Noise and Variance of the Noise) and 'Amplitude of SOI and SNOIs' are considered as input parameters for these three scenarios. These parameters are used as input to obtain optimum element weights, $\mathbf{w}_{opt}$; where the optimum beam pattern shapes is achieved (the ratio of the main lobe to the side lobes of the beam pattern is high), the MSE between the array output and the reference signal, $\mathbf{d}(t)$ is minimized and the Signal-to-Interference Ratio (SIR) of the beam pattern is high. This does not always result in the beam pattern having a maximum beam in the direction of the desired signal but does yield the array output signal with high SIR. Most often, this is accomplished by forming nulls in the directions of interfering signals. The step-size, $\mu$ is set to the value of 0.001, Mean of Noise and Variance of the Noise are set to 0 and 0.1, respectively. In practice, the input signal often contains white 'Gaussian' noise which has zero mean and constant variance. Thus, we assume a zero-mean noise and a small positive constant variance of 0.1.

The magnitude of the AF is normalized so that the peak of the AF is unity (3D simulation result) or 0 dB (2D simulation result). In this simulation, the AF will be set to -40 dB as the minimum level of threshold as the visibility of the main lobe and side lobes as the desired and the undesired pattern could be achieved within this range. The number of data samples are set to 500 iteration samples. The weight, $\mathbf{w}$ determines the amplitude and phase which produces the radiation pattern. The behavior of the radiation pattern shows the strength and direction of the desired/interfering signal in the system. In the simulation of the LMS algorithm in MATLAB software, there is one SOI at the angle of arrival from a single satellite and multiple SNOI (interference signals) at the side lobe part.

The normalized weight (amplitude), $\mathbf{w}$ and phase excitation coefficient (in degrees), $\beta$ output parameters of Scenario I case are plotted as in Figure 6 and Figure 7. The excitation of the antenna element at the highest point of 1.4 at the element number, $N$ of 53. During the simulation, random initial amplitude and phase excitation are present for each antenna element. Both are varied from each other since every element has different amplitude and phase distortions. The significant raised amplitude (amplitude error) excitation of the 53th array antenna element in Figure 6 contributes to the rise in sidelobes level in Figure 9 and Figure 10. However, the phase excitation for each array antenna element in Figure 7 are varies stepwise (or uniformly) with no phase distribution error and does not contributes to the rise in sidelobes level. This is due to the selection of the inter-element spacing between the array antenna element itself, which happen to be 0.5λ. The effect of the uniform phase excitation is the beam can be steered away from the broadside. This is an advantage as the main beam can be scanned towards the desired direction, electronically.

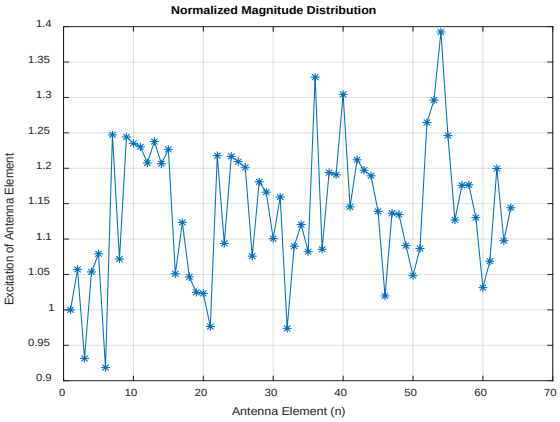


Fig. 6. Normalized weight (amplitude), w plot (scenario I).

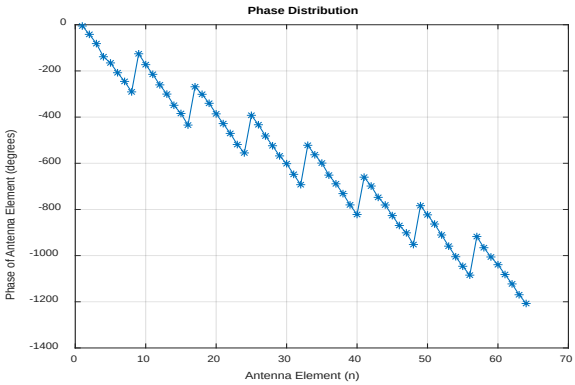


Fig. 7. Phase excitation coefficient (in degrees), $\beta$ plot (scenario I).

To analyze the ability of the algorithm which give a maximum gain in the direction of SOI and while placing null in the direction of SNOI, simulations were performed by applying the value of different interference signal directions with the three different real-time scenarios. By referring to the input parameters in Table 1, the 2D AF rectangular beam pattern plots (at azimuth and elevation angle) of SOI and SNOI are shown in Figure 8(a), Figure 8(b) and Figure 8(c) for Scenario I, II and III, respectively. The Signal-to-Interference Ratio (SIR) is defined as the ratio of the desired signal power to the undesired signal power. The red lines in Figure 8 (a) (b) (c) indicates the elevation and azimuth angle mark for the 2D azimuth plot describing the targeted satellite. The SIR values are derived by using Equation (17) as follows:

$$SIR(dB) = 10log\frac{Main\ lobe\ signal,S}{Total\ of\ interference\ signal} \quad (17)$$

The 2D AF rectangular plots of radiation pattern for Scenario I in Figure 8 (a) shows the value SIR of the main beam to the first side lobe about 7.8 dB at the elevation angle of 28°. In Scenario II and III, the SIR simulated results are 22.2 dB (el = 89°) and 19.75 dB (el = 47°). From this result, Scenario II produces the highest SIR compared to the SIR results from Scenario I and III.

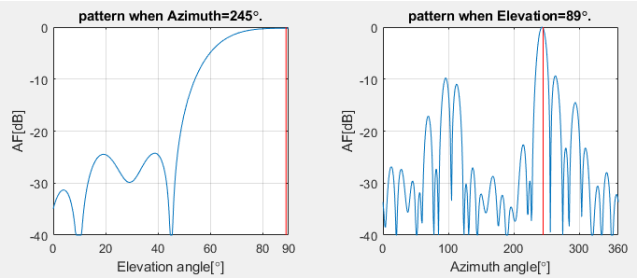


(a) Scenario I.

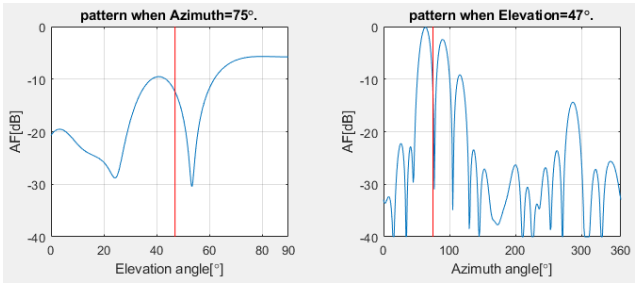


(b) Scenario II.

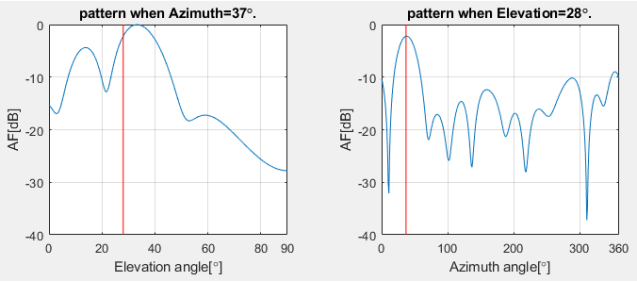


(c) Scenario III.

Fig. 8(a)(b)(c). 2D normalized AF of 64-elements planar array rectangular plots of SOI and SNOI for three different scenarios at azimuth and elevation angle view during CubeSats at maximum elevation.

The intensity distribution of the AF beam pattern towards the other side lobes for all three different scenarios when CubeSats reached the maximum elevation are as shown in Figure 9 (a), (b) and (c). Figure 9 (a) (b) (c) shows detail information about Figure 8 (a) (b) (c) including the 2D-intensity distribution viewed from the top of 2D-AF beam pattern for all three different scenarios. The red asterisk on the main beam peak indicates the position of targeted/tracked satellite.

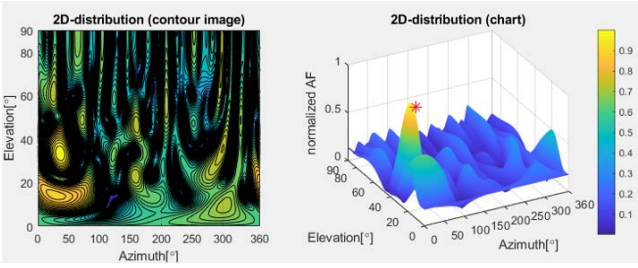


(a) Scenario I.

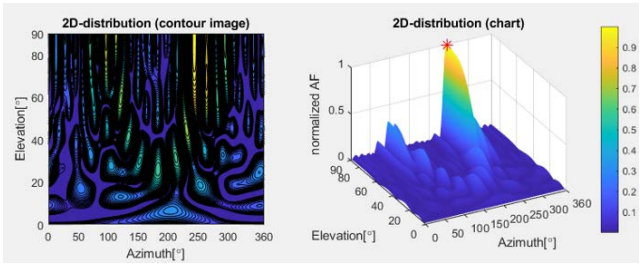


(b) Scenario II.

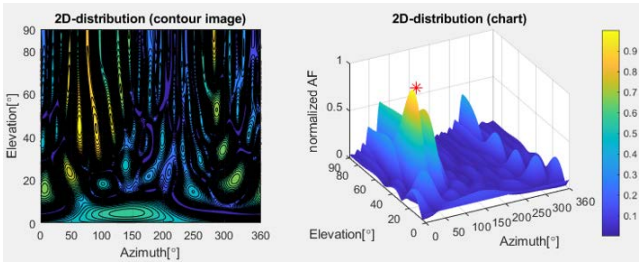


(c) Scenario III.

Fig. 9(a)(b)(c). 2D normalized AF beam pattern intensity distribution of 64-Elements planar array for three different scenarios at azimuth and elevation angle view during CubeSat reached maximum elevation.

The implementation of LMS algorithm shows the ability to track a desired satellite passes (within AOS and LOS) for three different scenarios, while minimizing side lobes of other interference satellites, simultaneously. In the real implementation of the AAA, the exact position of each satellite can be identified as they are emitting some satellite ID (also called a header) which can be predicted in advance by using SATPC32 software. As soon as the satellites reach the GS footprint, the training sequence or pilot signal (BPSK signal in this case) is sent by the GS to identify the satellite signal. Pilot signal is sent in proper timing to ensure that satellites acknowledge that the GS is ready for tracking, transmit and receive data. After finding the targeted satellite to be tracked, the main beam pattern is optimized in order to improve the SIR and produces an optimum beam pattern. In the simulation in Figure 10(a)(b)(c), the targeted satellite is tracked every 2.5 seconds with the optimum beam pattern. From the 3D beam pattern steering simulation results for the Scenario I, II and III in Figure 10 (a) (b) and (c)(i), the beam patterns are started producing some unwanted beams and rapidly steered towards random target at initial state (as soon as satellite reached AOS). The magnitude of the initial pattern is determined by the initial (arbitrary) choice of weights, $w$ . This interference phenomenon causes the beams field being cancelled or doubled simultaneously where it reduces the side lobes levels besides narrowing the main lobe [4]. The main beam direction is then steered to track the desired satellite (as satellites move and change its elevation and azimuth as in Figure 10 (a) (b) (c) (ii). As steering process of beam pattern is continued, side lobes started to appear as soon as satellite reached maximum

elevation as shown in Figure 10 (a) (b) (c) (iii). The LMS algorithm calculates a new main beam pattern for the satellite position 2.5 seconds later. To calculate the new beam pattern for the new satellite position, it takes maximum of 0.3 seconds on a laptop computer equipped with CPU Intel Core i7 8$^{th}$ Gen which cost about 1,000 USD. By referring to the Figure 10 (a) (b) (c) (iv), the side lobes power level is reduced simultaneously at the unwanted direction (side lobes reduction process). Finally, the targeted satellite reached LOS (as in Figure 10 (a) (b) (c) (v)) and the main beam pattern level is reduced and side lobes are randomly produced. The magnitude of the final pattern is determined by the strength of the interfering signal and the noise in the system. Training sequence or pilot signal is a known reference or desired signal, d(t) that transmitted a series of bits, periodically by the transmitter which are known in advance at the receiver. Figure 10 demonstrates that as the training sequence or pilot signal (BPSK signal) is corrupted by the noise in the environment (interference from nearby satellites), the adaptive arrays will then adjust the weights and steer the null of the array in the direction of the interferer satellites. As the iterative process progresses, the magnitude pattern will change to null out the interfering signal (from the interferer satellite direction) and focus on the SOI (from the targeted satellite). The convergence of the algorithm depends on the input parameter, step-size value, $\mu$ which controls the rate of adaptation. From this LMS algorithm simulation, the main beam pattern exhibits the capability of changing its main beam towards targeted moving satellite in every 2.5 seconds within the AOS and LOS. The three scenarios of 3D beam pattern steering changes are as plotted in Figure 10 (a), (b) and (c).

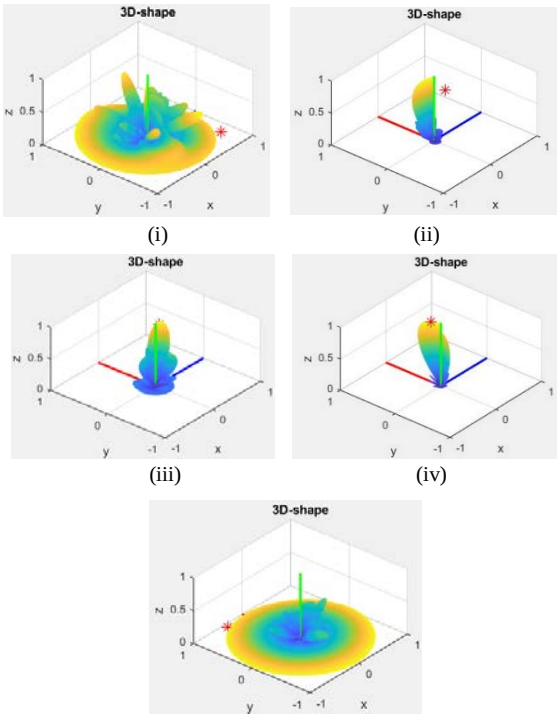


(i) (ii)

(iii) (iv)

(v)

(a) Scenario I.

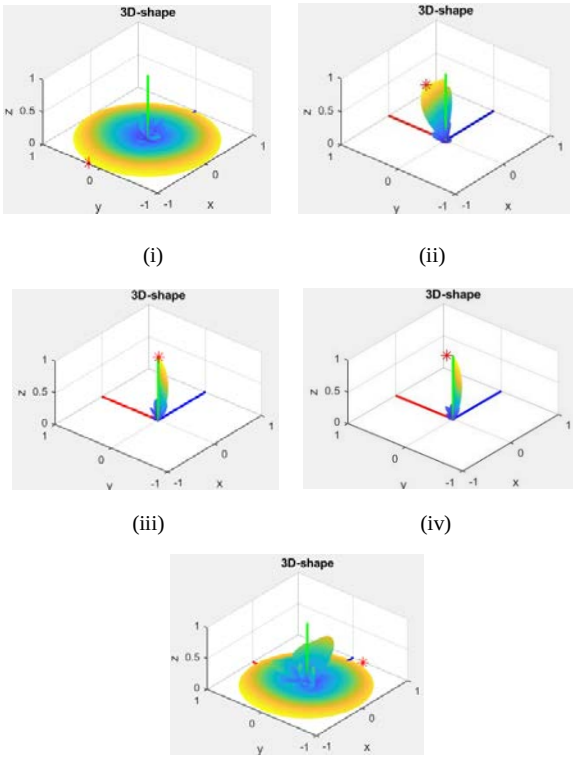


(i) (ii)

(iii) (iv)

(v)

(b) Scenario II.

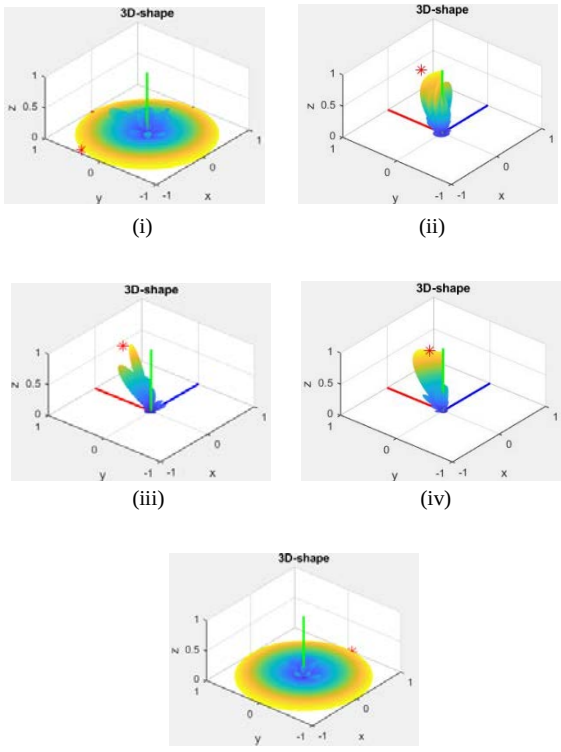


(i) (ii)

(iii) (iv)

(v)

(c) Scenario III.

Fig. 10(a)(b)(c). 3D beam pattern steering plot of 64-elements planar array for three different scenarios from AOS, maximum elevation and LOS.

In the principle of beamforming, a signal processing technique is implemented into combining array antennas in such a way that signal in a particular angle experience constructive interference (maximize the desired beam) while other signals will experience destructive interference (minimize the unwanted beam). From 3D simulation result for three scenarios in Figure 10, the LMS algorithm shows the ability to suppress side lobes (interference signals from interferer satellites) by putting nulls and steer the main beam towards the desired signal (targeted satellite). The output of (SIR) is maximized and the MSE is minimized as much as possible. Scenario II produces the narrowest main 3-dB beam width, followed by Scenario III and Scenario I. MSE is similar to SNR except that it accounts for interference in addition to noise power. The acceptable MSE values of each transmitting ($T_x$) and receiving ($R_x$) are evaluated to verify the link is operating as expected. The LMS algorithm simulation run of 500 iterations with parameters as in Table 1 resulted in an error plotted as in Figure 11 and Figure 12. Figure 11 shows the LMS planar array antenna MSE against iteration plot while the weight estimation error against iteration generated plot is as in Figure 12. MSE (as stated in Eq. 12) is the expectation error signal (unknown signal) and weight estimation error (as mentioned in Eq. 11) is weights that need to be find in order to minimize the expected error signal, MSE between the desired output of the array and the actual output of the array. By referring to the plot in Figure 11, MSE has hesitation at the beginning of iterations with an approximately maximum value of 0 dB and approach the average MSE value of -30 dB along the 500 iterations. An MSE of zero means that the estimator predicts observations of the planar array antenna weight parameter with perfect accuracy (ideal), but it is typically not possible as it started at 0 iteration. The weight estimation error is ranging from -17.5 dB to -43 dB (average weight estimation value is -30 dB) at iterations from 0 to 500 as shown in Figure 12.

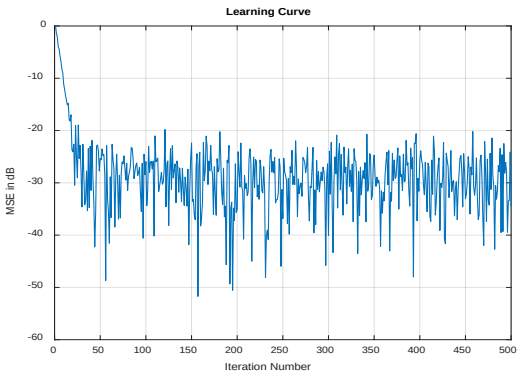


Fig. 11. MSE plot at each iteration.

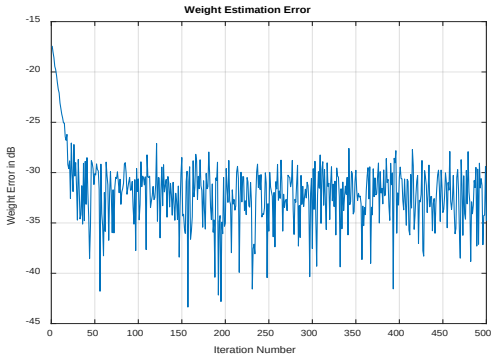


Fig. 12. Weight estimation error plot at each iteration.

## 6. Conclusion

This paper described the implementation of LMS algorithm in the AAA control system to have a reliable GS tracking control system. It can be utilized for satellites precise control tracking, instead of depending on the conventional big dish antenna with the manually controlled system. The implementation of AAA with electronically steerable beam scanning for satellite tracking system in a GS is the most promising solution to mitigate of the effect of multi-path fading and interference from surrounding/other satellites. Furthermore, it provides better coverage by improving the link quality and hence increase the capacity. By referring to the above-obtained MATLAB simulation results, the maximum radiation pattern (beamforming pattern) received at the appropriate angle toward appropriate satellite. Thus, it was concluded that the implementation of the LMS algorithm in AAA is suggested to be adapted in GS tracking control system to replace the conventional GS. As most of the small constellation satellites builders and researchers recently did a lot of research work on the AAA, there are still some technical challenges due to the high cost and massive scale of building the whole architecture within a short period.

## Acknowledgment

We would like to thank all the BIRDS partners, especially Center for Satellite Communication UiTM for supporting this development. We also would like to extend our appreciation to BIRDS-2 team members who helped to complete this project.

## References

1) Mendoza, H. A., Corral-Briones, G., Ayarde, J. M., & Riva, G. G.: Spectrum Coexistence of LEO and GSO Networks: An Interference-Based Design Criteria for LEO Inter-Satellite Links, In Computer Conference (CLEI), XLIII Latin American, 2017.
2) Salas Natera, Miguel & G. Aguilar, Andrés & Cueva, Jonathan & Fernández, J.M. & Padilla, P & Trujillo, J & Martínez, Ramón & Sierra Perez, Manuel & De Haro, Leandro & Sierra-Castaner, M.: *New Antenna Array Architectures for Satellite Communications*, *IntechOpen Limited, London,* **7** (2011), pp. 167-194.
3) Balanis, C. A.: Antenna Theory: Analysis and Design (Fourth Edition), John Wiley and Sons, Inc., Canada, 2016, pp. 931–980.
4) Kyun, N. C., Abdalla, A. G. E., Noordin, N. K., Khatun, S., Ali, B. M., & Sahbuddin, R. K. Z.: Modelling and Simulation of Phased

Array Antenna for LEO Satellite Tracking, International Conference on Information Networking ICOIN 2002, Cheju Island, Korea, 2002.
5) Hu, M., Tang, W., & Cai, C.: A new Variable Step-Size LMS Adaptive Filtering Algorithm for Beamforming Technology, Antennas Propagation and EM Theory (ISAPE), 2010 9th International Symposium, Guangzhou, China, 2010.
6) Ali, W. A., Mohamed, D. A., & Hassan, A. H.: Performance Analysis of Least Mean Square Sample Matrix Inversion Algorithm for Smart Antenna System. In Antennas and Propagation Conference (LAPC) 2013, Loughborough, United Kingdom, IEEE Paper, 2013, pp. 624-629.
7) Das, S.: Smart Antenna Design for Wireless Communication using Adaptive Beam-Forming Approach, TENCON 2008-2008 IEEE Region 10 Conference, Hyderabad, India, IEEE Paper, 2008, pp. 1-5.
8) Kamboj, S., & Dahiya, R.: Adaptive Antenna Array for Satellite Communication Systems, Proceedings of the International Multi Conference of Engineers and Computer Scientists, Hong Kong, 2008.
9) Lian, K. J.: Adaptive Antenna Arrays for Satellite Personal Communication Systems, Ph.D. Thesis, Virginia Polytechnic Institute and State University, 1997.
10) Breslin, D. F.: Adaptive Antenna Arrays Applied to Position Location. Master of Science's Thesis, Virginia Polytechnic Institute and State University, Blacksburg, 1997.
11) https://www.space-track.org/#tle